2015 American Control Conference
Palmer House Hilton
July 1-3, 2015. Chicago, IL, USA

Maximally Secure Mitigation of Protection Misoperations in Power Systems

N. Eva Wu, Qiu Qin, and Mustafa Salman

Abstract— **Protection misoperations have been recognized as a main culprit in causing cascading failures in modern power systems. This paper introduces the processes of misoperations and their mitigation into a scalable stochastic discrete-state model. In this framework, a mitigation strategy is developed to minimize the risk of cascading failures. The risk is quantified by a set of security indices that formally incorporate the uncertain knowledge of the continuous-state of rotor angles/speed deviations and the discrete-state of equipment faults. The security indices serve as mitigation criteria for selection of protection control actions. Real-time security evaluation poses a significant challenge because of the fraction-of-a-second response time required of protection functions. Two problems addressing this challenge are formulated and solved through a novel application of the phasor measurement units (PMUs)–their input samples in time-domain, rather than their output samples in phasor-domain, are used as redundant feedback variables. These time-stamped input waveform samples are processed to isolate transmission line faults in the presence protection false trips, and track the generators' rotor angles and speed deviations without invoking the swing dynamics. The computational issues and results are explained through a WSCC 3-generator 9-bus test system.**

I. Introduction

Protection misoperations fall into two broad categories: failure to trip and false trip, where trip means the opening of a (set of) switch(es) to remove a piece of supposedly faulty equipment from a power system. Because a typical protection system is rightfully designed to be dependable (to trip whenever it should) at the expense of security (not to trip whenever it should not) [21], false trips in a stressed system, which have been referred to as hidden failures[22], occur over 20 times more often than failures to trip [20]. A system can become stressed due an equipment fault, a change in load/generation power, or a severe event of nature.

Despite the efforts to *analyze* the impact of protection misoperations [22], [23], [28], and to *prevent* them from occurring by using adaptive relaying [23], [3], the alarmingly high rate of protection false trips is currently the top reliability concern of North American Electric Reliability Corporation (NERC) [20]. Other than some guidelines on simple mechanisms of recloses of circuit breakers [12] in response to disturbances, research on systematic protection asset management capable of *recovery* from false trips in the presence of a permanent fault in a transmission system remains an uncharted territory.

Recovery from protection misoperations presents a significant challenge because of the absence of a scalable mathematical representation encapsulating false trip and recovery processes from a traditional reliability model that typically only captures equipment failure and restoration processes. This work is the first to introduce a scalable mathematical representation of false trip and recovery processes into a reliability model. It builds on a stochastic framework proposed by the first author in [26], [27] to tackle recovery from a protection misoperation through dynamic management of equipment redundancy. Redundancy management makes use of functionally redundant equipment and devices in a system, and is used here interchangeably with discontinuous control actions, or simply control actions, such as high-speed fault clearing, high speed reclosing, regulated shunt/series switching of reactive devices [15].

The challenge to recover also stems from the need for a dissimilar redundant source of information in the face of protection misoperations. This work capitalizes on the PMU technology to provide the redundant source of information in an unconventional manner. Typically, analog inputs to a PMU are 3-phase currents and voltages at the secondary windings of instrument transformers. They are filtered to prevent aliasing, then converted into digital signals at tens of samples per ac cycle. The samples are time–tagged with a sub-microsecond accuracy according to the GPS clock. The samples are processed to produce positive-sequence voltage and current phasor estimates at a reporting rate of 30–120 output samples per second [21]. These are the so-called synchrophasors. The current IEEE standard [13], however, does not specify requirements on PMU responses to power system transients. This work abandons steady-state sinusoidal notions such as phasors and impedances, and processes directly the input waveform samples of PMUs instead to isolate transmission line faults and to track generator rotor dynamics.

Mitigating protection misoperations can be regarded as a switched system issue [8], as the admissible control actions in this case are most commonly actuated through switches, such as circuit breakers. The existing study of switched systems seeks to analyze or construct switching sequences for stability and other control objectives with a specifically defined notion of asymptotic stability [17], [18]. The nature of solutions sought here, however, is to establish transient stability [15] particular to a power system after the system has entered a transiently unstable configuration induced by an uncontrollable triggering event. The challenge here is to

N. Eva Wu and Qiu Qin is with the Department of Electrical and Computer Engineering, Binghamton University, Binghamton, NY 13902. They are supported by New York State Energy Research and Development Authority (NYSERDA) under Contract #30733. evawu@binghamton.edu, qqin@binghamton.edu

Mustafa Salman is currently pursuing his Ph.D degree in Binghamton University and supported by Turkish Military Academy during this work. Turkish Military Academy, Ankara, 06654, TURKEY, msalman1@binghamton.edu

978-1-4799-8684-2/$31.00 ©2015 AACC

do so before the holding time to cascading failures expires, which is typically a small fraction of a second and is dictated by the prevailing nonlinear system dynamics. Such an issue has not been touched upon in the switched system literature.

For the purpose of clarity in defining the scope of this paper, given many interpretations of the term security, the definition of reliability by NERC is adopted. It contains two functional aspects: adequacy (ability to provide uninterrupted service), and security (ability to withstand large disturbances). Thus reliability in this context is an overarching measure encompassing both steady-state availability (adequacy) defined for a discrete state stochastic process and transient stability (security) defined for a continuous state dynamic system whose mode of operation is determined by the prevailing discrete state. The fact that *availability* and *security* have been viewed as largely disconnected is evidenced by the two separate bodies literature in the power system community [24], [4]. This issue is recognized in less than a handful of publications [25], [27].

The paper is organized as follows. In section II, a scalable discrete state stochastic model is built to quantify the reliability impact of a protective control strategy, which is captured in a set of security indices specialized to avoidance and recovery from protection false trips. Section III uses the WSCC 3-generator 9-bus system [2] to explain the real-time computational issues for the security indices, which involve tracking the generators' electro-mechanical state with nonlinear least-squares and diagnosing faults with multiple-model filter banks [19]. The system is subject to random three-phase-to-ground short circuit faults in its transmission lines as well as relay misoperations. Three PMUs are placed at the terminal buses of the 3 generators in the system. Section IV concludes the paper.

II. A SECURITY-CENTRIC FRAMEWORK FOR MITIGATION OF PROTECTION MISOPERATIONS

A. A scalable stochastic model for inclusion of protection misoperation and recovery processes

Consider the availability model of an N-1 secure power system, which is planned so that system transient stability is maintained upon the prompt removal of a single piece/group of equipment after the onset of a critical fault in the equipment. It contains $N+2$ states: an aggregated pre-fault state p, N degraded but operational states, $d_1, \cdots, d_i, \cdots, d_N$, each corresponding to a post-fault state upon the removal of the equipment experiencing a critical fault[1], and an aggregated outage state o exceeding an economic impact threshold, at which a major restoration is required. System restoration is faced with a different set of challenges [1], and is outside of the scope of this paper. An analytic expression for system availability is derived in [27], and is shown to be increasing in each of the N security indices. The indices enter the availability model as the conditional probabilities of success

[1]A critical fault inevitably leads to a system outage in the absence of an appropriate protective control action.

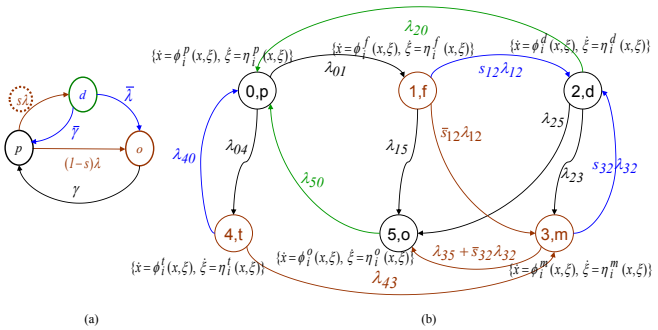

Fig. 1. (a) A rate transition diagram with the N N-1–secure states aggregated into a single degraded state d, resulting in an equivalent availability model with less detailed state information; (b) A 6-state aggregated rate transition diagram with protection misoperation and recovery processes included.

in diverting the system into one of the N N-1–secure states upon the occurrence of a critical fault.

To include misoperation and recovery processes in a simple model, an equivalent 3–state model is depicted in Fig. 1(a), where the N N-1–secure states in [27] have been aggregated into a single degraded state d, for which the system availability can be expressed as

$$A_s = \frac{\gamma\bar{\lambda} + \gamma\bar{\gamma} + s\lambda\gamma}{\lambda\bar{\lambda} + \gamma\bar{\lambda} + \gamma\bar{\gamma} + s\lambda\gamma + \bar{s}\lambda\bar{\gamma}}, \tag{1}$$

where λ, $\bar{\lambda}$, γ, and $\bar{\gamma}$ are state transition rates, and s is a conditional probability indicating the certainty of fault diagnosis and the likelihood of transient stability. It is named a security index because of its relation to transient stability. The monotonic dependence of availability A_s on the equivalent security index s observed in [27] is retained in this aggregated model.

Each of the three states in the aggregated model in Fig. 1(a) is now split into two to allow the observation of protection misoperation and recovery processes. More specifically, the pre-fault state is split into pre-fault (0 or p) and pre-fault false trip (4 or t), the degraded state is split into fault-on (1 or f) and N-1–secure (2 or d), and the system outage state is split into misoperation fault-on (3 or m) and system outage (5 or o). The new 6-state model is shown in Fig. 1(b). For an N-1–secure power system, discrete states p (or 0), d (or 2), and t (or 4) are to be called secure states hereafter, at which transient stability holds for the continuous-state dynamics. States f (or 1) and m (or 3) are insecure states as they are transiently unstable. State o (or 5) alone is called an outage state.

Table I contains a list of discrete state transition rates that are representative for the WSCC 9-bus system [2] shown in Fig. 2. This system is to be examined more closely in the next section.

At any given moment of time, a power system of any size and complexity resides in one of the 6 states in the Markov chain depicted in Fig. 1(b) with a holding time distribution $Prob[T_i \le t] = 1 - e^{-\Lambda_i t}$, where Λ_i is the total outgoing transition rate from state i, $i = 0, 1, \cdots, 5$. For example, $\Lambda_2 = \lambda_{20} + \lambda_{23} + \lambda_{25}$. Upon entering state i, the evolution of continuous state vectors (x, ξ), representing generator rotor

TABLE I

ENTRIES OF RATE TRANSITION MATRIX $Q = [q_{ij}]$

Transition from state i to state j	Transition rate q_{ij} (1/hour)	Security of action	Average inter-event time
Pre-fault (0) to fault-on (1)	$q_{01} = \lambda_{01} = 1/24/7/k$	not controllable	k week(s), fault arrival
Pre-fault (0) to misoperation (4)	$q_{04} = \lambda_{04} = \lambda_{01}$	not considered	k weeks(s); false trip
Fault-on (1) to post-fault (2)	$q_{12} = s_{12}\lambda_{12}, \lambda_{12} = 60^3/2/k$	s_{12}	$2k$ ac cycles, protection trip
Fault-on (1) to false-trip fault-on (3)	$q_{13} = \bar{s}_{12}\lambda_{12},$	$\bar{s}_{12} = 1 \quad s_{12}$	false trip
Fault-on (1) to system outage (5)	$q_{15} = \lambda_{15} = 60^3/10/k$	not controllable	$10k$ ac cycles, fail to trip
Post-fault (2) to normal (0)	$q_{20} = \lambda_{20} = 1/k$	not considered	k hour(s), restoration
Post-fault (2) to false trip fault-on (3)	$q_{23} = \lambda_{23} = 1/24/k$	not considered	k day(s), false trip
Post-fault (2) to system outage (5)	$q_{25} = \lambda_{25} = \lambda_{01}$	not controllable	Second line short
False trip fault-on (3) to post-fault (2)	$q_{32} = s_{32}\lambda_{32}, \lambda_{32} = 60^3/6/k$	s_{32}	$6k$ ac cycles, recovery
False trip fault-on (3) to outage (5)	$q_{35} = \bar{s}_{32}\lambda_{32} + \lambda_{35}, \lambda_{35} = \lambda_{01}$	$\bar{s}_{32} = 1 \quad s_{32}$	Fail to recover/2nd line short
False trip pre-fault (4) to normal (0)	$q_{40} = \lambda_{40} = 60^3/6$	not considered	$6k$ ac cycles, recovery
False trip pre-fault (4) to (3)	$q_{43} = \lambda_{43} = \lambda_{01}$	not controllable	k week(s), 2nd line short
System outage (5) to normal (0)	$q_{50} = \lambda_{50} = 1/24/k$	not considered	k day(s), restoration

Transitions with zero rates ($q_{ij} = 0$) are not included. Also not included in the table are the diagonal entries of Q, which are: $q_{00} = \lambda_{01} \quad \lambda_{04}$, $q_{11} = \lambda_{12} \quad \lambda_{15}$, $q_{22} = \lambda_{20} \quad \lambda_{23} \quad \lambda_{25}$, $q_{33} = \lambda_{32} \quad \lambda_{35}$, $q_{44} = \lambda_{40} \quad \lambda_{43}$, and $q_{55} = \lambda_{50}$.

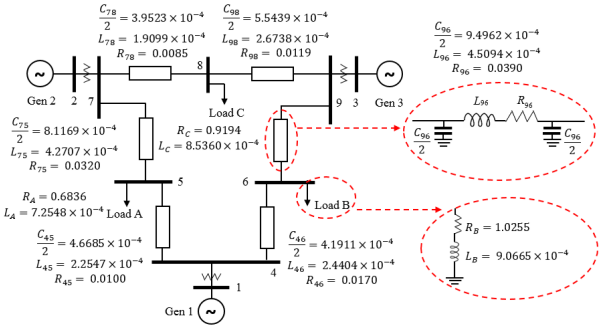

Fig. 2. One-line diagram of the WSCC 3-generator 9-bus system [2]; all time-domain circuit parameters are derived from the corresponding 60 Hz impedances in pu on a 100-MVA base.

dynamics and electric dynamics of the transmission network, respectively, is governed by a pair of differential equations from the set $\{\dot{x} = \phi^i(x,\xi), \dot{\xi} = \eta^i(x,\xi)\}$ particular to discrete state i. Set notation $\{.\}$ signifies that if state i is aggregated, it can have multiple continuous state dynamics associated with it. The dimension and the content in (x,ξ) depend on the prevailing system configuration.

Despite its simplicity, the 6-state model contains the essential information necessary for imposing computational and technological requirements. The model can be utilized to study protection misoperations for a power system of any size and complexity. Transition rates associated with failure and misoperation events generally increase linearly with the system size as dictated by the Poisson superposition property [5]. The following two examples reveal some aspects of utilities of the scalable low resolution model.

Example 1. Event probabilities. The event probability that the system enters the N-1–secure state d given that the current state is f (a critical fault has occurred) is given by

$$Prob[d|f] = \frac{s_{12}\lambda_{12}}{\lambda_{12} + \lambda_{15}}. \tag{2}$$

Security index s_{12}, a conditional probability, quantifies the degree to which a protection function is effective. Similarly, the event probability that the system recovers to the N-1–secure state d is, given that current state is m in which a protection misoperation has occurred while a critical fault is on is given by,

$$Prob[d|m] = \frac{s_{32}\lambda_{32}}{\lambda_{35} + \lambda_{32}} \approx s_{32}. \tag{3}$$

Again security index s_{32} encapsulates the effectiveness of the recovery process.

Example 2. System availability and sensitivity to security. Denote state probability distribution of the stochastic model in Fig. 1(b) by $\pi = \begin{bmatrix}\pi_0 & \pi_1 & \pi_2 & \pi_3 & \pi_4 & \pi_5\end{bmatrix}$. The following Chapman-Kolmogorov equation governs the dynamics of the discrete state probability distribution:

$$\dot{\pi}(t) = \pi(t)Q, \quad \pi(0) = \begin{bmatrix} 1 & 0 & 0 & 0 & 0 & 0 \end{bmatrix}, \tag{4}$$

$$Q = \begin{bmatrix} q_{00} & \lambda_{01} & 0 & 0 & \lambda_{04} & 0 \\ 0 & q_{11} & s_{12}\lambda_{12} & \bar{s}_{12}\lambda_{12} & 0 & \lambda_{15} \\ \lambda_{20} & 0 & q_{22} & \lambda_{23} & 0 & \lambda_{25} \\ 0 & 0 & s_{32}\lambda_{32} & q_{33} & 0 & \bar{s}_{32}\lambda_{32} + \lambda_{35} \\ \lambda_{40} & 0 & 0 & \lambda_{43} & q_{44} & 0 \\ \lambda_{50} & 0 & 0 & 0 & 0 & q_{55} \end{bmatrix}.$$

A first order approximation of the system's unavailability, $\bar{A}_s = \pi_5 = 1 - A_s$ for the 6-state model solved from $\pi Q = 0$ and $\sum_i \pi_i = 1$, can be derived as

$$\bar{A}_s \approx \frac{\lambda_{01}}{\lambda_{50}} \left(1 - \frac{s_{32}\bar{s}_{12} + s_{12}}{(1 + \frac{\lambda_{25} + \bar{s}_{32}\lambda_{23}}{\lambda_{20}})(1 + \frac{\lambda_{15}}{\lambda_{12}})}\right) \pi_0, \tag{5}$$

where practical knowledge of disparate transition rates (Table I) is made use of, and $\pi_0 \approx 1$ can be assumed for any functioning power system. The monotonic dependence of availability on security remains true. With $s_{12} = 0.7$, introducing a perfectly effective recovery strategy from nil would reduce the system unavailability to $25\% = \bar{A}_s(s_{32} = 1, s_{12} = 0.7)/\bar{A}_s(s_{32} = 0, s_{12} = 0.7)$.

The above method of remodeling is applicable to the higher resolution model in [27], which contains N degraded states for N critical faults. Splitting each of its states yields a discrete state-space formed from the direct product of a composite set of binary equipment states $\{faulty, degraded\}$ and a composite set of binary relay states $\{restrain, operate\}$, respectively. Thus the 6-state

model in Fig. 1(b) is expansible systematically to any desired resolution.

With the new scalable stochastic model, the objective and scope of this paper can be further clarified: mitigation of protection misoperations amounts to developing a realizable real-time strategy for reliable and speedy transitions out of states f and m into state d so as to minimize the likelihood of entering the system outage state o.

B. Continuous state dynamics during the holding times of discrete states at fault-on misoperation and post-fault

Some transitions in Fig. 1(b) or in Equation (4) can be influenced through systematic decision and control with real-time information feedback. These are called controllable transitions. Two of the controllable transitions are considered. At the fault-on state f, a protection misoperation occurs when the outgoing transition falsely trips into misoperation state m (or fails to trip and thus enters outage state o,) instead of correctly tripping into degraded secure state d. Thus the concern on the high rate of protection false trips is reflected in the need to raise security index s_{12} to be closer to 1. At misoperated state m, a protection misoperation occurs when the outgoing transition fails to recover into state d, and enters outage state o instead. Thus the concern on the largely absent systematic recovery scheme from a misoperated protection system is reflected in the need to raise s_{32} (from nearly 0) to as close to 1 as possible.

Since a false trip from f to m is also faced with the issue of recovery from m to d once m is entered, the following development focuses on the recovery process from m to d, unless issues particular to transitioning out of f arise that call for a separate analysis.

With the narrowed focus on studying recovery from misoperated state m to N-1–secure state d, only the relevant power system dynamics among all expressed in Fig. 1(b) are duplicated below.

$$\{\dot{x} = \phi^m(x,\xi),\ \dot{\xi} = \eta^m(x,\xi)\},\ t_m < t < t_d \qquad (6)$$

$$\{\dot{x} = \phi^d(x,\xi),\ \dot{\xi} = \eta^d(x,\xi)\},\ t_d \leq t < \infty. \qquad (7)$$

The notations above are partially borrowed from [24] with two main differences. (i) [24] considers only the electro-mechanical state x, whereas (6) and (7) consider also the electric network state ξ. The fast dynamics of ξ matters, however, only in diagnostic tasks. (ii) [24] considers a configuration change (discrete state transition) from fault-on ($\dot{x} = \phi^f$) to post-fault without modeling protection misoperations, whereas (6) and (7) consider a configuration change from a misoperation after the arrival of a fault to a degraded secure (post-fault) state with a possibly imperfect recovery scheme. Though a misoperation can occur with or without a fault, the case of a misoperation without a fault is omitted as it leads to a N-1–secure state with ample time for a recovery.

Since the holding time at state d is typically much longer than that in state m, the latter is assumed to last till an infinitely remote future to simplify the discussion of transient stability and the definition of a stability region. Note, however, the problem setting of this paper does not preclude the discussion of sequential events before the system settles into a post-fault stable equilibrium.

Denote the stability region [24] (region of attraction) of a post-fault system around its stable equilibrium by

$$A(x^e,\xi^e) \equiv \{(x,\xi) | \lim_{t\to\infty} (\psi^d(x,\xi,t), \mu^d(x,\xi,t)) = (x^e,\xi^e)\},$$

where $(\psi^d(x,\xi,t), \mu^d(x,\xi,t))$ is the post-fault continuous state governed by (7) initiated at (x,ξ). Since the transient stability of the power system is defined for the slower electro-mechanical dynamics, the two coupled differential equations $\dot{x} = \phi^d(x,\xi)$ and $\dot{\xi} = \eta^d(x,\xi)$ can be replaced by a differential-algebraic system $\dot{x} = \phi^d(x,\xi)$ and $0 = \eta^d(x,\xi)$ to allow elimination of component ξ in the differential equation. From now on, the variable ξ is suppressed in the discussion of stability region $A(x^e)$ and transient stability.

The classical endeavor [24] has been to compute x using the fault-on electro-mechanical dynamics and characterize the boundary $\partial A(x^e)$ of $A(x^e)$ based on the post-fault electro-mechanical dynamics in real-time, in order to answer if $x \in A(x^e)$. Our new endeavor deals with a protection false trip during a fault at insecure discrete state m, where the continuous state dynamics defined by $\{(\dot{x} = \phi^m,\ \dot{\xi} = \eta^m)\}$ is unstable.

III. Security indices as real-time mitigation criteria

The formal definition of s_{32}, the information required for its computation, and its relation to diagnosis, estimation, and control of the underlying dynamic power system are now elaborated. The discussion that follows is applicable to defining and computing s_{12}, or any security index associated with a controllable transition one wishes to introduce.

For the sake of clarity in the subsequent development, four assumptions are (re)stated. (i) The system under study has been planned to be N-1–secure, which meets the current NERC standard. (ii) A protective action removes at most one piece of equipment at any given time. Thus any equipment removal decision must be preceded by a reinstatement of a previously removed piece of equipment. (iii) The system has the knowledge of the protective control action taken and the time of the action (t_m or t_d), whereas it relies on the mitigation strategy to isolate an equipment fault and its onset time (t_f). (iv) PMUs are networked through fiber-optic links so that concerns on channel capacity, data transfer rates, and electro-magnetic immunity are eliminated from the discussion here.

The WSCC 9-bus model [2] is used to explain the computational and other technological issues involved. The system one-line diagram is shown in Fig. 2. In the following discussion, the system is assumed to have constant circuit parameters. In particular, The transmission lines are modeled as Π–circuits, and each load is modeled as a constant resistance and inductance in series. The internal equivalent inductances for generators 1, 2, and 3 are 0.0608 pu, 0.1198 pu, and 0.1813 pu, respectively. Only transmission line faults of the three phase to ground type are considered, and fault

locations are the mid-points of the transmission lines. Three PMUs are located at buses 4, 7, and 9 with fiber-optic links in between them.

A. Fault diagnosis based on PMU input samples and electric network dynamics

Suppose there are N critical equipment faults in an N-1–secure system. Together with pre-fault and system outage states, the total number of modes to isolate is $N+2$ in order to render a transition decision from m to d, or from f to d, given that the state of protection system is known. This number reduces to $N+1$ if outage mode is excluded, as millisecond-scale urgency is no longer an issue at state o. Denote by $\{f_0, , f_1, \cdots, f_N\}$ the N+1 operation modes to distinguish among pre-fault mode f_0 and faulty mode f_i, $i = 1, 2, \cdots, N$. Note that discrete states and modes are two different sets, because a fixed mode f_i may be related to one of many possible fault-on states corresponding to different protective control actions. Let

$$p(t) = (p_{f_0}(t), p_{f_1}(t), \cdots, p_{f_N}(t)) \tag{8}$$

be a snapshot at time t of the mode probability distribution as the outcome of a real-time fault diagnosis process. Sufficiently high rate of measurement samples must be used because of the required speed in protection asset management at an insecure state (m or f), where a diagnosis decision typically must be reached within a fraction of a second after the onset of a critical fault. This work exploits the potential of the PMU input samples acquired by the current, potential, or capacitive voltage transformers and time aligned based on the GPS clock among remote estimates.

Fault diagnosis example. A multiple-model filtering approach [19] built on the electric network dynamics is used to identify the system mode. The 3-PMU network enables redundant protection functions. The generator output voltage waveforms calculated based on the measurement signal model (9) serve as the input variables in the state-space electric network model, whereas the PMU input waveforms serve as the output variables in the network state-space model. Note that the electric network dimension changes as its configuration changes. During the diagnosis process, only those filters of possible system modes corresponding to the prevailing protective control action are activated. Thus the filter bank varies as the protective control action evolves over time. Fig. 3 shows the structure of filter banks. A sample path of a fault diagnosis outcome is shown in Fig. 4, where the isolated modes are aggregated to match the low resolution discrete state defined in Section II-A. It is seen that using electric network dynamics can provide highly accurate and fast diagnosis outcome in the presence of protection misoperations.

B. Post-fault regions of attraction estimation

Let $J_{f_i,u}(x)$ be the characteristic function defined on an estimated post-fault region of attraction provided by one of the control actions u in admissible set $\mathcal{U} = \{u_1, \cdots, u_M\}$. Despite the significant advancement in both theories and

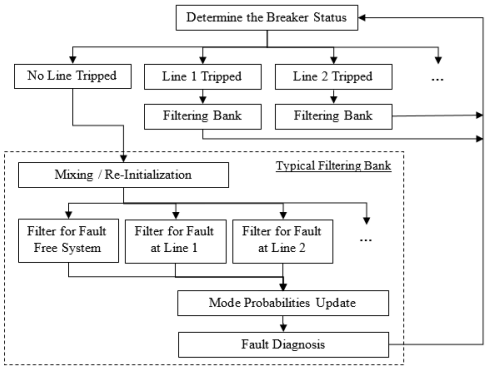

Fig. 3. A set of parallel banks of multiple model filters is built for each protective control action. Parameters of the electric network are assumed known. It is assumed that the three branch currents and the bus voltages at buses 4, 7, and 9 are measured because of the assumed PMU locations. Only one bank is activated at any given time. The active bank is determined by the protective control action taken.

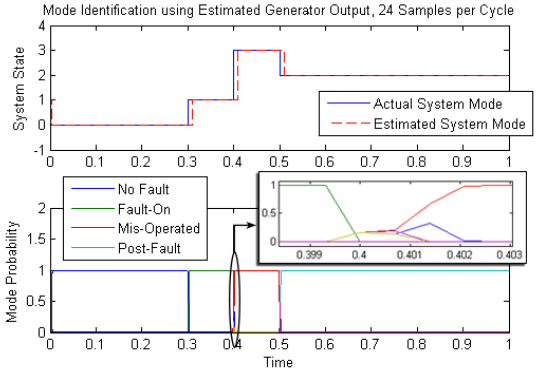

Fig. 4. The PMU input waveforms are sampled at 24 samples/cycle with signal to noise ratio at 15dB. The system starts with a normal operation at state '0'. A mid-point short to ground fault in line 5-7 occurs at 0.3 sec (state '1'). Line 7-8 is falsely removed at 0.4 sec., which renders the system enter insecure state '3' (m). The fault is cleared at 0.5 sec. by reconnecting line 7-8 and removing line 5-7 (state '2' (d)). The recovered system enters and stays at state d (post-fault) from 0.5 sec. till the end of the simulation. Based on the operation of breakers, three banks of filters are used. The first set of filters, which consists of a normal design model and 6 design models for 6 line faults, runs from 0 to 0.4 sec. The second and third sets of filters, which consist of a post-fault design model and 5 misoperated design models, run from 0.4 to 0.5 sec and 0.5 to 1.0 sec, respectively. Note that only the 4 dominant mode probabilities are indicated in the legend, while a total of 19 filters are used during the diagnosis process.

numerical techniques over a period of several decades, region of attraction estimates remain a great computational challenge. The regions of attraction of the WSCC 9-bus are estimated using both the closest UEP method [6], and an off-line simulation method. Characterization of the regions of attraction for the N post-fault modes of an N-1–secure system is treated as an off-line task based on energy functions in this paper. Its relation to security index is revealed in (10).

C. Tracking the electro-mechanical states with PMU inputs

Let $f_{(\hat{x})}(t, x)$ be a snapshot at time t of the probability density function for the estimate of electro-mechanical state $x = (\delta, \omega)$. The distribution can be estimated by formulating a maximum likelihood problem [9], [14]. More specifically, this paper considers using PMU input samples at generators' terminal buses to estimate the magnitudes, frequencies, and phases of the generator internal voltages, which are modeled as quasi-steady-state sinusoidal sources. Since measurement

data samples are locally acquired, no data communication issues arise.

Rotor state tracking example. Suppose a PMU is installed at the terminal bus of generator j of the system in Fig. 2, $j = 1, 2, 3$, so that the bus voltage waveform $v_j(t)$ and the current waveform $i_j(t)$ injected from the generator are both sampled and time-stamped. Let L_j be the sum of the internal subtransient inductance of generator j and the leakage inductance of its step-up transformer. The following nonlinear signal model can be used to estimate the generator rotor angle, speed deviation, as well as the internal voltage magnitude.

$$\begin{aligned} y_j(k) &\equiv v_j(k\Delta t) + L_j \frac{i_j((k)\Delta t) - i_j((k-1)\Delta t)}{\Delta t} \\ &= E_j(k) cos(\omega_0 k\Delta t + \Delta\omega_j(k) k\Delta t + \phi_j(k)) + \epsilon_j(k) \\ &\equiv h_j(x_j(k)) + \epsilon_j(k), \end{aligned} \tag{9}$$

where $x_j(k) = (\Delta\omega_j(k), \phi_j(k), E_j(k))$. The second line of (9) makes use of the knowledge that the generator internal voltage is quasi-steady-state sinusoidal, which allows us to implement the nonlinear least-squares estimator with an extended Kalman filter [9], without invoking swing dynamics of the system. Using the PMU inputs for estimation, some preliminary results are shown in Fig. 5, where voltage and current measurement samples are generated using a Simulink model with 2nd order classical models for the generators. Estimations of $x_j(k)$ using PMU outputs (synchrophasors) are also showed in Fig. 5 for comparison. Note that the measurements are acquired at 24 samples per nominal AC cycle and the window length of 24 samples is used for obtaining the PMU outputs. The common 24 sample/cycle output rate is used to ensure a fair comparison, though it is much higher than a typical synchrophasor report rate of, say, 60 samples/sec.

D. Security index as a criterion for misoperation mitigation

Define coverage [26] of fault i associated with mode f_i present at misoperation state m

$$c_{f_i,u}(t) = \int_x J_{f_i,u}(x) f_{(\hat{x})}(t, x) dx, \tag{10}$$

where $c_{f_i,u}(t)$ is the probability that the system enters a post-fault mode associated with control action $u \in \mathcal{U}$ exerted at time $t > t_m > t_f$. t_f is the fault onset time, and t_m is the false trip time. Note that control action at t_d is intended to recover from a false trip. Thus $t_d - t_m$ is the holding time the system spends at the most recent insecure mode at discrete state m. The holding time must be smaller than a critical clearing time, beyond which no admissible control actions can establish a stability region to enclose the departing state $\psi^m(x, \xi, t)$.

Because coverage is discounted by the imperfection of outcomes of diagnosis which aims to identify the prevailing critical fault, a security profile associated with control u is defined as follows [27].

$$s_{f_i,u}(t) = p_{f_i}(t) c_{f_i,u}(t), \tag{11}$$

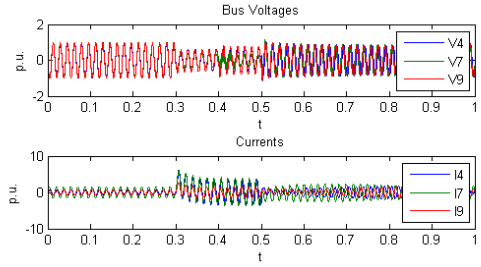

(a) Measured terminal voltage and current waveforms

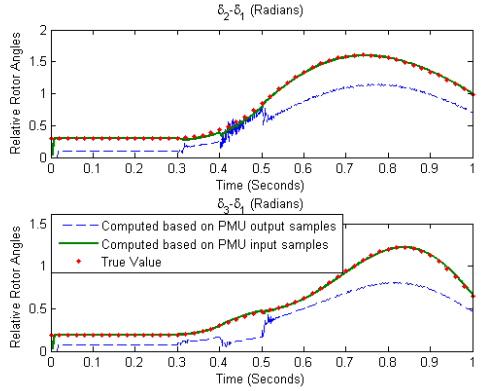

(b) Estimated relative rotor angles

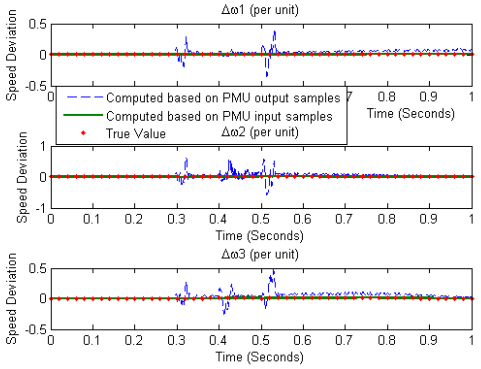

(c) Estimated rotor speed deviations

Fig. 5. The electro-mechanical states of the three generators are estimated using PMU inputs and outputs. This estimation algorithm does not involve any swing dynamics. The system starts with a normal operation. A mid-point short to ground fault in line 5-7 occurs at 0.3 sec. into the simulation. Line 7-8 is falsely removed at 0.4 sec., which renders the system enter insecure state m. The fault is cleared at 0.5 sec. by reconnecting line 7-8 and removing line 5-7. The recovered system enters and stays at state d (post-fault) from 0.5 sec. till the end of the simulation.

where $p_{f_i}(t)$ is the estimated mode probability. Control action and action time u and t_d can be determined by tracking $s_{f_i,u}(t)$ in real-time until it exceeds a prescribed threshold, and satisfies

$$\max_{i \in \{0,\, 1, \cdots, N\}, u \in \mathcal{U}} s_{f_i,u}(t) > s_{th} \tag{12}$$

persistently for a period of time up to t_d. At t_d, the optimal control action

$$u^* = \arg\max_{u \in \mathcal{U}} s_{f_{i^*},u}(t_d) \tag{13}$$

is applied. When all faults are aggregated, $s_{f_{i^*},u^*}(t_d) = p_{32}(t_d) c_{32}(t_d) \equiv s_{32}$ is now named security index in relation to the recovery from a false trip in the scalable stochastic process. Thus (13) defines a maximally secure mitigation strategy. Apparently, this strategy minimizes the risk of

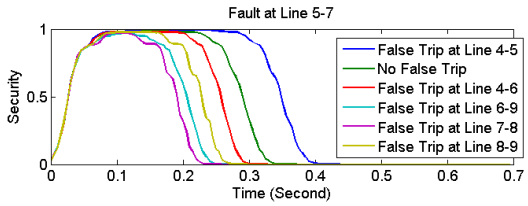

Fig. 6. Coverage profiles evaluated using (10), where a mid-point short to ground fault in Line 5-7 has occurred. All but one profiles represent misoperations where a line is falsely tripped (instantaneously at the onset of a fault $t = 0$), and the system recovers from the false trip at time t. Since there is no ambiguity and hardly any delay in the diagnosis outcome as seen in Section III-A, recovery, i.e., reinstatement of line 7-8 and removal of line 5-7, can be securely performed within a window of about 40 ms after 80 ms into a misoperation, according to the information provided by the purple profile. Thus recovery from a false trip is real-time achievable.

cascading failures from p to f to m to o. In general, the definitions and analyses above hold for $s_{12}(t)$, and for any security profile associated with a controllable transition in the discrete state model in Fig. 1(b).

Coverage profiling example. Six post-fault regions of attraction, corresponding to the removal of each of the six transmission lines, are computed off-line via simulations for the system in Fig. 2. The color coded curves in Fig. 6 are coverage profiles evaluated using (10) with an assumed normally distributed state tracking error. A mid-point short to ground fault in Line 5-7 has occurred. All but one profiles represent misoperations with a line falsely tripped at the onset of a fault ($t = 0$), and the recovery from the false trip occurs at t when a corrective control action is taken.

The profiles in Fig. 6 indicate that the opportunity for recovery from state m (misoperation fault-on) to state d (degraded but N-1–secure) is almost as good as having a correct trip from state f to state d. The larger window corresponding to the false trip of Line 4-5 is attributed to the complete loss of Load A.

IV. Conclusions

New developments are made in three areas. (i) Misoperation and recovery processes are incorporated into a scalable stochastic model where security indices capturing the avoidance and recovery of protection false trips enter as computable conditional probabilities; (ii) Real-time computation of such conditional probabilities is tackled by using the PMU input samples and electric network dynamics, which abandon the convention of computation in the phasor-domain, assuming that post-fault regions of attraction are obtainable off-line; (iii) A mitigation strategy maximizing the security indices associated with protective control actions is put forward, which extends the idea proposed in [27] to dealing with mitigation of protection misoperations.

Because of the extreme complexity of the mitigation problem at hand, many simplifying conditions have been assumed in this paper. Knowing these conditions constitutes another contribution of the paper that is to be able to define a rich set of future research problems. In summary, the study finds that the realization of the proposed mitigation strategy is within our reach provided that current technological and computational potentialities are fully exploited.

References

[1] M.M. Adibi and L.H. Fink, Overcoming restoration challenges associated with major power system disturbances, *IEEE Power and Energy Magazine*, pp.68-77, 2006.

[2] P.M. Anderson, A.A.Fouad, *Power System Control and Stability,* 2nd edition, IEEE Press, 2003.

[3] E.E. Bernabeu, J.S. Thorp, V. Centeno, Methodology for a security/dependability adaptive protection scheme based on data mining, *IEEE Transactions on Power Delivery,* vol. 27, pp.104-111, 2012.

[4] R. Billinton, and R. Allan, *Reliability Evaluation of Power Systems*, Plenum Press, 1996.

[5] C. G. Cassandras, and S. Lafortune, *Introduction to Discrete Event Systems*, 2nd Edition,Springer, 2008.

[6] H.-D. Chiang *Direct Methods for Stability Analysis of Electric Power Systems: Theoretical Foundation, BCU Methodologies, and Applications*, Wiley, 2011.

[7] H. Chiang and L. Fekih-Ahmed, Quasi-stability regions of nonlinear dynamical systems I: fundamental theory and applications, *IEEE Transactions on Circuits and Systems,* vol. 43, pp. 627-635, 1996.

[8] R. Decarlo, M. Branicky, S. Pettersson, and B. Lennartson, Perspectives and results on the stability and stabilizability of hybrid systems, *Proceed- ings of the IEEE,* vol.88, pp. 1069-1082, 2000.

[9] A. Gelb, Editor, *Applied Optimal Estimation,* MIT Press, 1988.

[10] M. Hale and Y. Wardi, Mode Scheduling under Dwell Time Constraints in Switched-Mode Systems, *Proc. American Control Conference,* 2014.

[11] N.G. Hongorani, and L. Gyugyi, *Understanding FACTS: Concepts and Technology of Flexible AC Transmission Systems*, IEEE Computer Society Press, 1999.

[12] IEEE PES Relaying Committee, *IEEE Guide for Automatic Reclosing of Circuit Breakers for AC Distribution and Transmission Lines (IEEE Std C37.104^{TM}-2012)*, IEEE Standards Association, 2012.

[13] *IEEE Standard for Synchrophasors for Power Systems, C37.118-2005,* Sponsored by the Power System Relaying Committee of the Power Engineering Society, 2005.

[14] S. Kay, *Fundamentals of statistical signal processing: estimation theory*, Prentice-Hall, 1993.

[15] P. Kundur, *Power System Stability and Control*, N.J. Balu, & M.G. Lauby, Editors, McGraw-Hill, 1994.

[16] X.-R. Li and Y. Bar-Shalom, Multiple-model estimation with variable structure, *IEEE Transactions on Automatic Control* vol. 41, 1996.

[17] D. Liberzon and A. Morse, Basic problems in stability and design of switched systems, *IEEE Control Systems Magazine*, vol.19, 1999.

[18] H. Lin and P. Antsaklis, Stability and stabilizability of switched linear systems: A survey of recent results, *IEEE Transactions on Automatic Control,* vol.54, pp. 308-322, 2009.

[19] D. Magill, Optimal adaptive estimation of sampled stochastic processes, *IEEE Transactions on Automatic Control*, vol. 10, 1965.

[20] North American Electric Reliability Corporation, Report on State of Reliability 2013.

[21] A.G. Phadke, and J.S. Thorp, *Synchronized Phasor Measurements and Their Applications,* Springer, 2008.

[22] J.D.L. Ree, Y. Liu, L. Mili, A.G. Phadke, and L. DaSilva, Catastrophic failure in power systems, causes, analysis, and counter measures, *Proceedings of the IEEE*, vol.93, pp.956-964, 2005.

[23] S. Tamronglak, S. E Horowitz, S. E Horowitz, and J. S. Thorp, Anatomy of power system blackouts: preventive relaying strategies, *IEEE Transactions on Power Delivery,* vol.11, pp.708-715, 1995.

[24] P. Varaiya, F. F. Wu, and R. Chen, Direct Methods for Transient Stability Analysis of Power Systems: Recent Results. *The Proceedings of the IEEE*, vol.73, pp.1703-1715, 1985.

[25] F. F. Wu, and Y. Tsai, Probabilistic Dynamic Security Assessment of Power Systems: Part I - Basic Model. *IEEE Transactions on Circuits and Systems*, vol.30, pp.148-159, 1983.

[26] N. E. Wu, Coverage in fault-tolerant control, *Automatica*, vol.40, pp.537-548, 2004.

[27] N. Eva Wu, and Matthew C. Ruschmann, Fault-tolerant control of power grids for security and availability, *Proc. American Control Conference,* 2012.

[28] F. Yang, A.P.S. Meliopoulos, G.J. Cokkindes, and Q.B. Dam, Bulk power system reliability assessment considering protection system hidden failures, *2007 iREP Symposium - Bulk Power System Dynamics and Control - VII, Revitalizing Operationl Reliability*, 2007.